1 SEISMIC SAFETY ANALYSIS OF THE OLD PORTUGUESE CATHEDRAL IN SAFI,
2 MORROCCO
3
4

5 Luís F. Ramos
6 *Assistant Professor, ISISE, University of Minho, Guimarães, Portugal, lramos@civil.uminho.pt*

7

8 Thomas Sturm
9 *PhD Student, ISISE, University of Minho, Guimarães, Portugal, tsturm@civil.uminho.pt*
10
11
12

13 **ABSTRACT**
14
15 The paper presents the main results of the safety analysis of the Safi Cathedral. First a general

16 description of the cathedral and the restoration project are given. To assess the safety of the main arch

17 of this cathedral after the restoration, a seismic line of thrust analysis was used. The results of this

18 uncommon analysis for structures which face seismic hazard were then compared to the results

19 obtained from a phased pushover analysis. The results of the seismic line of thrust analysis turned out

20 more conservative than those of the finite element analysis, although in both cases the results depend

21 on the modeling hypothesis.

22 **KEYWORDS**: Seismic analysis, thrust line analysis, pushover analysis, sonic tests, FE model

23 **1. INTRODUCTION**

24 The city of Safi is located in the West African coast, about 150 km from the city of Marrakesh,

25 Morocco. The Cathedral of Safi was the first Portuguese cathedral constructed outside Portugal during

26 the discoveries period, which started in the 15th C. and lasted until the beginning of the 17th C., and is

27 an outstanding example of the *Manueline* architecture. The construction of the cathedral was

28 completed during the decade of 1520 (Campos, 2007). It was originally a three nave church and is

29 believed to be similar to other cathedrals such as the Ponta Delgada and the Funchal Cathedral in the

30 Madeira island, Portugal (Ramos et al., 2010). After 1540, the cathedral was occupied by Muslims

31 who significantly changed the use and the construction. The space of the naves was used to add

32 several residential buildings and the altar was turned into a hammam (bathhouse for women in Arab).

1 The only original parts of the structure that remain until today are the main altar, crowned by a ribbed

2 vault, the lateral chapel, whose roof is missing, and one outside wall that stands alone.

3 The cathedral will soon be submitted to a structural intervention that will convert the compound into a

4 museum space. The project includes the preservation of the original remains of the cathedral, the

5 correction of existing problems in the structure and the improvement and installation of new

6 infrastructure to support tourism and cultural events. Therefore, safety conditions and the conservation

7 of the built heritage must be assured. This paper describes briefly the Cathedral of Safi and its

8 restoration project. Then, the seismic hazards of this region are characterized and analyzed. Finally, a

9 *Seismic Line Of Thrust Analysis* (SLOTA) of the main arch and a phased pushover finite element

10 analysis of the cathedral is presented.

11 **2. THE SAFI CATHEDRAL**

12 During the 15th C., Safi was an important trading port between Europeans and Africans. Between the

13 years 1488 and 1541, Safi was governed by Portuguese and by the name of Safim. Amongst the

14 Portuguese constructions from the *Manueline period* which still remain and stand out are the Cathedral

15 of Safi, the Castle of the Sea and the Fortress of Safi.

16 The Cathedral of Safi was the first cathedral constructed beyond continental Portuguese borders.

17 Similarities with other Portuguese cathedrals constructed during that period, such as the cathedral of

18 Ponta Delgada and of Funchal (Campos, 2007), can be admitted. A comparison between the remains

19 of this cathedral and the Funchal Cathedral has already been presented in Ramos et al. (2010). The

20 cathedral is located in midst of the medina of Safi, as can be seen in Figure 1.

21 The Cathedral of Safi was constructed and finished during the decade of 1520 by Master-builder João

22 Luís under the promotion of archbishop D. João Subtil. The Cathedral was occupied by Muslims,

23 which transformed the altar into a hammam. In Campos (2007) and historians of art's opinion, the

24 vault of the main altar of the Safi Cathedral, with exception of constructions in the military field,

25 remains the masterpiece of *Manueline architecture* subsisting outside of Portugal.

After 1541, with the ascension to power of Sultan Cheikh and the retreat of the Portuguese from Safi, a mosque was built next to the Safi Cathedral. Thus, the Cathedral is located in a place of high historical, religious and social value for the city of Safi.

2.1 Description of the Safi Cathedral

The remaining structure of the Safi Cathedral is the main altar, the right lateral chapel and an exterior wall. The main altar is almost squared and is crowned by a ribbed vault. Its dimensions are approximately 8.2 m x 7.8 m width in plan, with a maximum height of 9.7 m measured from the existing pavement to the center of the vault. The lateral chapel is also rectangular with approximately 4.5 x 5.4 m width in plan and 6.9 m high walls. This part of the structure is exposed to the outside since its former vault does not exist anymore, although the bottom parts of the ribs still remain. The external wall is 15.1 m long, 9.6 m high measured from the inside of the compound and 8.2 from the outside. The thickness is uniform with 0.85 m of width.

Because the cathedral was built in the same period as the Funchal and Ponta Delgada cathedrals, it is believed that the Safi Cathedral had a similar structural organization. In this case, the Safi cathedral would have been an arrangement of three naves and two lateral chapels, covered by a light wooden roof. Figure 2.a shows the actual structural configuration of the remaining Cathedral and the adjacent structures. Figure 2.d shows the present plan configuration of the Funchal Cathedral. Figure 2.b shows the probable original plan configuration of the Safi Cathedral, based on the layout of the Funchal Cathedral.

Figure 2.c shows an elevation of what is thought to be the original remains of the main altar with its ribbed vault and the lateral chapel without roofing. It also can be appreciated in this figure that the level of the alley is 1.4 m higher than the pavement of the Cathedral. This is very usual in old cities, since the cities have been built up progressively over time. Therefore, streets and alleys are mainly composed of infill material which has accumulated over centuries. Finally, these old streets and alleys can be up to some meters over the level of the former ground floors.

1   Figure 3 shows some general views of the inside of the main altar. As it can be observed in Figure 3.a,

2   the structure is maid of two types of stone masonry. The walls are of masonry with limestone units and

3   lime mortar joints. Nevertheless, several joints with cement mortar could be observed, which probably

4   correspond to recent reparation works. The vault of the main altar has ribs made of granite stones with

5   joints of poor lime mortar. The remaining walls correspond to porous limestone.

6   The inner space, shown in Figure 3.c, corresponds to the place were the hammam was installed after

7   the Portuguese left Safi. The narrow door that can be observed on the left side leads to the lateral

8   chapel and to the exit of the cathedral, and is the only entrance to the main altar today. On Figure 3

9   also modifications introduced by the Muslim community can be observed. These modifications

10   correspond to the closing of the windows with masonry, as shown in Figure 3.a and Figure 3.b. Also

11   the space beneath the arch of the north-west elevation was closed with a masonry infill wall, as seen in

12   Figure 3.c. This part is believed to have been completely open towards the main nave under the

13   Portuguese rule. A detail of the encounter of the arch, the column and the infill wall can be observed

14   in Figure 3.d.

15   In Figure 4 general aspects of the Cathedral are shown. The alley that limits with the compound of the

16   cathedral is shown in Figure 4.a. On the left side the exterior wall of the cathedral and on the right side

17   the exterior wall of the Grand Mosque of Safi can be seen. The exterior wall of the lateral chapel is

18   shown in Figure 4.b. The narrow entrance from the alley to the cathedral is shown in Figure 4.b and

19   Figure 4.c. A difference between the level of the street and the pavement of the ground floor of the

20   cathedral can be observed. In Figure 4.d, the lateral chapel is shown. The view is in the north-west

21   direction in which the naves of the cathedral once stood. This arch was not closed with a masonry

22   infill wall like the arch of the main altar was.

23   **2.2   Seismicity in Safi**

24   The territory of Morocco is subjected to substantial seismicity, since it lies in the zone of influence of

25   the collision between two continental plates, the African Plate and the Eurasian Plate. Figure 5.a

26   shows a world map with the major continental plates and the location of Morocco.

1   As it can be seen in Figure 5.a, at the west of the Strait of Gibraltar Morocco is influenced by the

2   activity of the Açores-Gibraltar midocean ridge which divides the Mid Atlantic from the North

3   Atlantic. This fault was responsible for the Lisbon 1755 earthquake, which caused extensive damage

4   and a destructive tsunami on the Atlantic shores. East of the Strait of Gibraltar, this region is under the

5   influence of the fault of the Alboran Sea which stretches itself from the north of Morocco in east

6   direction. This fault was responsible for the earthquake of 1522 which caused major destruction in the

7   northern zone of Rif and Fès (RPS2000, 2001).

8   The local soil has clay characteristics. Due to the local characteristics of the soil, a dynamic

9   amplification factor of 2 should be considered in case of the design of new stiff buildings (RPS2000,

10   2001). This was not considered in the structural analysis of the Safi Cathedral since, although it is

11   massive, this structure has been standing on site for more than four centuries. In this case, due to the

12   time period that has elapsed, the soil settlements of first and second order have already taken place,

13   making the soil stiffer. If local site effects are still active, is unclear.

14   Safi is located in the zone with the highest seismic magnitude in Morocco, according to the seismic

15   code of Morocco (RPS2000, 2001). The maximum peak ground acceleration is estimated in 0.16 g,

16   with a 10% of probability for a 50 years return period for the city of Safi. Figure 5.b shows the seismic

17   zonification of Morocco given by its seismic code.

18   This is in accordance with a study carried out by Benouar et al. (1996) about the seismicity of the

19   Maghreb region. The authors affirm that near Safi several earthquakes with magnitude Ms higher than

20   5 have taken place during the 20th century. The epicenters and their respective magnitude are shown

21   in Figure 6. They also defined a hazard map based on the return periods (in years) for seismic events

22   higher than 0.14 g, in which the location of Safi would have a return period of 400 years for

23   earthquakes with this magnitude. Since the code of Morocco considers a Peak Ground Acceleration

24   (PGA) of 0.16 with a return period of 50 years, it can be concluded that the code is on the conservative

25   side.

1 This argument is reinforced when analyzing the Hazard map provided by the USGS (2011) for Africa.

2 According to this map the zone of Safi would have a PGA between 0.04 and 0.08 g, with a 10%

3 probability of exceedance in 50 years for a 475 years return period. The maximum value of this range

4 is half of the one defined by Morocco's RPS 2000 code.

5 On the other hand the seismic code of Morocco defines a modification factor of the spectrum for

6 structures with a damping different than 5%. It amplifies the spectrum for damping lower than 5% and

7 it reduces it for damping over 5%. Since historic masonry has usually a damping coefficient higher

8 than 5%, the demand for the Safi Cathedral could be reduced. As an example, if the damping factor

9 would be 10%, the PGA would be reduced to 0.76 of its original value.

10 Finally, the distinction between "upgrading" and "improvement" of heritage building must be made.

11 While upgrading refers to "a group of works which aim to resist to the seismic actions adopting the

12 increasing of the resistance and/or the reduction of the effects of the seismic action", an improvement

13 refers to "the execution of works that concern the single structural element of the building with the

14 purpose of achieving greater safety without modifying in a substantial way the global behavior of the

15 building". This problem has been addressed by the Italian authorities through the OPCM 3274 (2003)

16 ordinance, since upgrading cultural heritage building to the seismic safety demands of today's codes is

17 virtually impossible in technical and/or economical terms. This code introduces the concept of

18 "controlled improvement". It does not require an upgrading to current seismic protection levels;

19 consequently it allows the reduction of the seismic design actions to asses the safety levels of

20 interventions, depending on the use and the importance of the building. Table 1 shows the reduction

21 factors defined by the code. This approach is useful in order to define the minimum intervention or

22 even the need for an intervention.

23 Based on the previous information and as discussed in Sturm (2010), the PGA that would result from

24 the use of Morocco's seismic code would be highly conservative and responds rather to design

25 purposes than to evaluating the real effects of a seism on a structure. In light of the arguments

26 exhibited before, a PGA of 0.16 g has been adopted as the seismic action to evaluate the intervention

1   of the Safi Cathedral. This value is not under conservative as the PGA's given by the USGS hazard

2   map, but it is also not over conservative as the values proposed by the RPS2000. It rather follows the

3   OPCM 3274 proposal of reducing the design seismic actions in case of a structure of irregular average

4   use (museum spays for presentations).

5   **3. VISUAL INSPECTION**

6   During the visual inspection, attention was only given to the original parts of the Cathedral, since the

7   surrounding structures are going to be demolished according to the existing rehabilitation project.

8   During the inspection no relevant cracks in the masonry walls which are going to be maintained were

9   detected. Some minor defects were detected in the intrados of the vault, which are connected with

10   earlier metallic strengthening interventions and vertical deflection, see Figure 7.a and b. The extrados

11   of the vault is covered with a cement layer that has large cracks, in which even vegetation grows, as

12   shown in Figure 7.c. This defect permits the infiltration of water, the washing out of fine material and

13   the deterioration of the lime mortar of joints of the vault and walls beneath. Some mortar joints of the

14   lower part of the walls of the main altar have been repointed with cement mortar. Figure 7 shows a

15   summary of the defects encountered.

16   The arch of the main altar, that is closed nowadays, presents an out-of-plane curvature in direction of

17   the former naves. Through the 3D survey with a laser scanner made by Miranda (2009), an out-of-

18   plane plumbing of approximately 30 cm was determined. The origin of this defect could correspond to

19   a construction defect, to the lateral thrust of the vault, or to a damage that was induced to the structure

20   when a shaft for the hamam was opened through the vault. Which one of these is the main or only

21   cause is unclear.

22   The walls and pavement of the main altar show some humidity. However, despite of the existing

23   humidity no efflorescence neither in pavement nor walls was detected which would indicate the

24   presence of water in the soil of foundation.

25   More details about this and other defects can be found in Ramos et al. (2010).

4. INVESTIGATION OF THE STRUCTURE

In order to obtain more information about the state of conservation of the Cathedral, sonic tests were carried out. Also a laboratory test was carried out to determine the type of mortar used originally in the construction of the cathedral. Since no major damage relating to cracks was observed during the visual inspection and the compression stresses are low (due to the thickness and low rise of the walls), flat-jack test was not carried out.

Only the main findings of the NDT tests are going to be mentioned in this work. More information can be found in Ramos et al. (2010).

4.1   Sonic tests

With exception of steel, the range of values of sonic velocities of construction materials is high, due to the dispersion of the quality and density of materials. Figure 8.a shows some average values for a variety of materials. In case of the Safi Cathedral, the sonic test was used to determine the state of conservation of the walls. Figure 8.b shows the location where the sonic test was carried out. The velocities were measured on a 40 cm horizontal and 30 cm vertical mesh. The transducers were positioned on opposite sides of the wall, permitting direct measurements. On each point, 10 measurements were taken from both sides.

Figure 8.c shows a velocity map of the mean velocities of propagation of the wall. The velocities measured ranged from 0.5 to 2.0 km/s, with a mean value of 1.1 km/s. The mean value corresponds to an expected value for old masonry walls, nevertheless the difference between the maximum and minimum values indicate the existence of cavities inside the walls. All indicates that the wall corresponds to a three leaf wall with smaller stones or gravel in its center. This was confirmed through observations made with help of a perforation on the external wall. It was also verified that the masonry has no stones which occupy the entire thickness of the walls.

4.2   Laboratory tests

Small samples of mortar and stones (approximately 5×5×5 cm) were taken from inside the wall by means of a borehole. These were then analyzed through X-Ray Fluorescence Spectroscopy to determine the inert/binder composition.

The results of these tests show that the mortar presents a content of 96.1% of binder and 3.9% of inert materials. Paying attention to the individual components, it can be confirmed that this mortar corresponds to a lime-mortar of high purity, with a usual inert/binder ratio for mortars used in historical constructions (Ramos, 2009). The results of the tests carried out on stones of the masonry indicate that these correspond to calcaric stones.

5.   DESCRIPTION OF THE RESTORATION PROJECT

The future restoration works are presented in order to give the reader a view of the changes which the Safi Cathedral will undergo. Special attention was put in the structural modification of the restoration project, which will be discussed next.

The restoration project of the Safi Cathedral aims at the creation of a new cultural space in the city of Safi. The modification consists in the demolition of some old structures and/or structural elements surrounding the original building and which do not correspond to the original cathedral. Also new structures will be incorporated. The idea is to create a public space which in its essence resembles what the original Safi Cathedral might have looked like, integrating harmoniously the original remains of the cathedral with the new structures, but making a clear distinction between them. Other cathedrals, such as the Funchal Cathedral or the Ponta Delgada Cathedral served as models for the conception of the restoration project.

The first step of the intervention project consists in installing scaffoldings inside the main altar which reach till the intrados of the vault to do a series of works. The main activities will consist in the removal of all metal clamps which were inserted into some ribs near the opening of the chimney in the past, the cleaning of the stones of the ribs and vault and the refurbishment of all joints of ribs and vault

1   which present deterioration. This instance will also be used to install a monitoring system of vertical

2   and horizontal displacement to control the structural works of the next steps.

3   The second step consists in the refurbishment of the lateral walls of the main altar. Since voids have

4   been detected with the sonic test, the injection of lime based mortar to consolidate the walls is planed.

5   Then, the walls will get cleaned and the cement mortar joints which were introduced as a repair at one

6   point in the past will be removed and repointed with lime mortar, and hence resemble its original way.

7   The third step corresponds to the removal of the biological agents and the concrete layer on the

8   extrados of the vault, which was described in the visual inspection.

9   The fourth step of the restoration project consists in demolishing several walls inside the compound,

10   see Figure 9.a. The removal of most of these walls does not affect structurally the original cathedral,

11   with exception of the infill wall of the main arch and an orthogonal wall which supports the section of

12   this arch, see Figure 9.a and c. These walls give in the present configuration a constraint to the original

13   parts. The influence of the removal of these walls on the original structure has already been studied in

14   Sturm (2010), concluding that the original structure can stand the removal of these walls during a short

15   period. Still, the construction of a lateral buttress is necessary to protect the structures from

16   earthquakes, see Figure 9.b. Even though it was already analyzed in Sturm (2010), this work

17   reassesses the structural safety of the cathedral after incorporating the changes of the restoration

18   project. This step was deemed necessary, due to the simplifications of the geometry and since some of

19   the future structural elements were incorporated as boundary conditions in the previous FE model.

20   These elements were incorporated explicitly in the new FE model. This work also complements the

21   previous work with a SLOTA.

22   The fifth step corresponds to the erection of columns and arches in the longitudinal direction, in

23   resemblance of the Funchal Cathedral (Ramos et al., 2010), forming the main and lateral naves. Since

24   the longitudinal walls are very slender and correspond to an interpretation of the original cathedral and

25   not a reconstruction, they will be made of reinforced concrete. This way the original parts will be

26   identifiable from the new elements. The longitudinal arches of the nave will rest directly on the

original structure, giving the buttresses an extra resisting load. A masonry gable between both arched walls will then be constructed on the upper part of the main altar arch to close this space, see Figure 9.b.

The sixth step consists in the removal of the infill wall under the main arch of the main altar, see Figure 9.c. This work will be executed slowly and with much care, in order to avoid the generation of damages in the rest of the structure. Vertical and horizontal displacements of the arch and the vault will be monitored constantly during this work. Additionally, a portion of the top of the external wall will be demolished to make space for the supports of the roof beams of the lateral nave.

Finally, as it can be seen in Figure 9.d, an infill on the vault and the wooden beams for the roofs will be placed on the main vault and the lateral nave. The new roofs will rest on these wooden beams. Then the arched walls will be connected by steel trusses and by rods placed above the arches. The naves will be covered with a light wooden roof, also in resemblance to the Funchal Cathedral.

6. SEISMIC LINE OF THRUST ANALYSIS

The graphical static method, which has been applied to masonry structures with arches and vaults, is based on the line of thrust theory. The line of thrust is the locus of the point of application of the internal forces or stress resultants. The graphical application of this theory was initially presented by Rankine in 1858 and then Culmann proposed to use this method systematically in 1866 (Heyman, 1998). The general approach of engineers in those times was that if a line of thrust could be drawn inside the middle third of the arch, the arch would be safe (Kurrer, 2008). Continuing this logic, if the line of thrust can be drawn inside the buttresses, the buttresses have the correct dimensions to withstand the lateral thrust. The drawback of this method is that an infinite number of solutions can be found, depending on the border conditions that are chosen. At the beginning of the 20th century, this method was the standard tool to check the stability of arches (Heyman, 1998). Even though the elastic theory was already developed at this point and seen as a more powerful tool since a unique solution could be found, it was impossible at that time to use it systematically to check or design structures because of the high numerical effort required.

1   A basic assumption of this theory is that the masonry is infinitely stiff and that it has infinite

2   compression strength. This can be regarded as valid if the mortar joints are thin enough to not allow

3   internal strains and since the compression stresses are normally low in historical masonry

4   constructions. Also, no displacements or sliding between the units are considered in this theory

5   (Heyman, 1966). If a line of thrust contained within the limits of the arch can be found, it proves that

6   the arch is stable. However, the arch does not necessarily work according to the solution found, since

7   the solution is not unique and could be working according to any other possible solution within the

8   arch. If the line of thrust is outside the middle third of an arch, this will produce tension forces on the

9   opposite surface of the arch in that section. Since tensile strength is not considered for masonry, a

10   crack would develop in this section. However, this does not mean that the arch is unstable.

11   In the thrust line theory, each time the thrust lines becomes tangent to the boundary of an arch, a hinge

12   will develop. If no thrust line can be found within the boundaries of the arch, the arch is unstable. If a

13   line of thrust can be found for a given external load which creates enough hinges to develop a

14   mechanism, the load corresponds to the lower bound of the ultimate state. This statement is called the

15   lower bound theorem. Further background of limit analysis can be found in Heyman (1995) and

16   Huerta (2008).

17   Usually, the Line Of Thrust Analysis (LOTA) has been applied to undeformed arch sections.

18   However, the line of thrust might be affected by previous large deformations or settlements of the

19   foundations of the structure (Huerta, 2008). To take into account these modifications, the modified

20   geometry can therefore lead to an improved analysis of the structure, as analyses in Block et al.

21   (2006a) show.

22   But what about the LOTA of structures in earthquake prone regions? Block et al. (2006b) propose a

23   modification of the classical approach of the LOTA adopted from Heyman (1995). These authors

24   make use of a common practice in structural engineering design which corresponds to simulate

25   earthquake loading by a constant horizontal force that is some fraction of the weight of the structure in

26   magnitude. This is also equivalent to applying a constant horizontal acceleration that is some fraction

1   of the acceleration of gravity. Their proposal for a *seismic line of thrust analysis* (SLOTA) is to tilt the

2   ground surface, and therefore the entire analyzed structure, by a given angle and then perform the

3   classical static LOTA. This will apply an effective vertical ground acceleration (gravity, g) and a

4   horizontal acceleration of $\lambda * g$. The relationship between the inclination angle of the ground surface

5   (α) and the seismic coefficient (λ) is given by $\lambda = \tan(\alpha)$. The tilting angle α can be increased

6   until the thrust line can not be contained within the structure. This will lead to the maximum seismic

7   coefficient the structure can resist. Figure 10.a shows an example of this method.

8   This equivalent pseudo-static SLOTA is conservative in that it assumes an infinite duration of the

9   loading, just as other equivalent static analysis do. But actual earthquake loadings are of much shorter

10 duration and could allow the structure to recover due to inertial effects. On the other hand it is

11 unconservative since it neglects the effects of crushing and sliding of blocks (Block, 2006.b).

12 Nevertheless, this method can be considered an important tool, since it is easy to use and depicts in a

13 graphic way the possible mechanism of collapse of a vaulted structure under earthquake loading. A

14 deeper study with tools, such as finite element models, might be necessary to complement this

15 analysis, especially in complex three dimensional structures.

16 This method has already been applied by Oikonomopoulou et al. (2009) to a section of the medieval

17 church of Our Lady of Burgh in Rhodes, in a similar fashion of that proposed by Block et al. (2006b).

18 An important remark made by the authors in this case was that a change of the critical points of hinge

19 formation can be observed between the structure subjected to lateral loading and the structure under

20 static loads. Moreover, the range of admissible horizontal forces in the side of the arches is much

21 smaller in the first case.

22 But tilting the structure can lead to confusion, since when a structure is tilted the gravity load (W) is

23 split into a component normal to the tilted plane ($W\cos(\alpha)$, that will represent the gravity load) and

24 one parallel to the tilted plane ($W\sin(\alpha)$, which represents the seismic loading). This would mean

1   that the parallel load (i.e. seismic load) would be equivalent to W when $\alpha = 90°$ and would not tend

2   to infinity as with $\lambda = \tan(90°)$.

3   To avoid any misinterpretation between the nature of the real structure and the method (SLOTA), the

4   authors proposes to use the same method, but to not tilt the structure. Keeping the weight (W) of the

5   structure constant and applying a horizontal load ($\lambda * W$). Since the LOTA is based on the sum of

6   vectors, the resultant force in the center of mass has a direction of an angle of α from the vertical

7   direction and $\lambda = \tan(\alpha)$. This is equivalent to use the LOTA with lines of action rotated by an angle

8   of α, which represent a seismic load of $\lambda * g = \tan(\alpha) * g$. Figure 10 shows an example of this

9   approach.

10   ## 6.1   Application to the Safi cathedral

11   In the case of the Safi Cathedral, one of the main concerns is the arch of the main altar, since the

12   restoration project foresees the demolition of its infill, the construction of a new buttress and the

13   placement of a masonry parapet on top of it. A static LOTA was already performed earlier (Sturm,

14   2010), but without taking into account the seismic loading this structure might face in future. In this

15   paper, the static LOTA as well as the SLOTA of this section of the cathedral is described. Only the

16   geometrical configuration after the restoration of the cathedral, and the extra weight on the main arch,

17   with and without buttress has been analyzed.

18   The SLOTA was done without tilting as described earlier. Since the possible configurations of the line

19   of thrust are virtually infinite as long as the lower bound is not reached, a software was developed by

20   Sturm (2011) to simplify this task. This software was programmed in Visual Basic and uses as input

21   the 2D geometry of the section, the thickness of each block, the weight density of the material, the

22   location of three critical points of the line of thrust in the arch and the angle of inclination of the

23   ground. The output consists of the graphical display of a structure with the equivalent SLOTA. The

24   analysis was performed by rotating the lines of action in both directions until only one line of thrust

25   within the boundaries of the arch could be found, condition which is necessary to comply with the

26   lower bound-theorem. However, it is difficult to determine if the lines of thrust found in the seismic

analysis really correspond to the "true" ultimate line of thrust. But in any case, it can be stated that the

results found are close enough, since the further the line of actions are rotated, the further the range of

possible solutions is narrowed down (Oikonomopoulou et al., 2009).

The results of this analysis are shown in Figure 11. As seen in Figure 11.a, in the static case, a line of

thrust can be found within the structure without incorporating the buttress. But it also can be observed

that in this case the range of possible lines of thrust is narrow and that the possible lines of thrust form

three hinges. This leads to the conclusion that if the buttress is not built, cracks at the ends on the

extrados of the main arch and in the middle on the intrados of the main arch might form. If the buttress

is taken into account, as seen in Figure 11.b, the range of possible lines of thrust in the main arch

widens, with lines of thrust which can pass near to the middle of the main arch. This would mean that

if the buttress is put in place before the infill is demolished, the arch might not experience, or may

experience smaller, cracks.

The seismic analysis in both directions is shown in Figure 11.c and Figure 11.d. The expected cracks

which will appear due to the formation of hinges are drawn with gray in a schematic manner. The

seismic coefficients which result without considering the buttress are very low, and therefore this

analysis was discarded. The seismic coefficient determined in the -X direction is of $\lambda = 0.275$ and of λ

$= 0.175$ in the +X considering the buttress. As mentioned in Oikonomopoulou et al. (2009), a change

of the critical points can be observed when compared to the static case, in which the critical point in

the middle moves to the left or right, forming new cracks in the intrados. It is also important to notice

that the seismic coefficients are different for both directions, being smaller for the +X direction. This

confirms that it is very important to make this kind of analysis in both directions in case of

unsymmetric structures. Regarding the appearance of possible new cracks, it is important to bare in

mind that previous cracks might influence the location of new cracks. This is not captured by this kind

of analysis.

The analysis can be considered conservative, since the walls in the orthogonal direction which meet

this section of the cathedral may have a positive impact on the lines of thrust, increasing the seismic

coefficient. It is also conservative because it does not take into account the ductility that these kinds of masonry structures have. This analysis demonstrates that the placement of a new buttress before demolishing the infill of the arch is mandatory, and that a conservative estimation of the ultimate seismic coefficient of this section is of 0.175 g. If this seismic coefficient is divided by the above defined demand of 0.16 g, a safety factor of 1.09 can be determined. This value is over 1.00, but can not be considerate satisfactory without a cross-examination with another method. It is important to point out that this safety factor is regarding the stability of the structure and does not take into account the material strength, since infinite compressive strength is assumed for masonry.

7. NONLINEAR PUSHOVER ANALYSIS

Although nonlinear time-history analysis is a powerful tool to asses the behavior and to predict the demand of a structure during an earthquake, some difficulties arise when using this method. The main disadvantages are due to the fact that time-history analysis requires a set of ground motion data (which are not available for all locations) and that it is very time consuming. And even though a ground motion set might be available, the results may not be equivalent to the demand the structure will undergo in earthquakes yet to come.

In replacement of the time-history analysis, the pushover analysis has been gaining acceptance in the last two decades. A pushover analysis is basically a non linear static analysis in which a structure is loaded stepwise with a given load pattern laterally. The lateral load patterns should approximate the inertial forces expected in the building during an earthquake (Lopez, 2004). Common used load patterns correspond to inverted triangular, uniform and modal shape distribution along the height of a building (Kalkan et al., 2004), as well as combined or adaptive load patterns (FEMA-356, 2000). This pattern is then incremented until a target displacement is reached or non convergence of the model is obtained. A target point (or node) must therefore be defined. Usually the target point is set on the last floor of the structure. It is important to mention that it has mostly been used to analyze multistory frame buildings, in which the lateral loads can be distributed in each level. However, the previous

mentioned patterns can also be applied in a continuum solid in which the mass is discritized along the height.

Once the analysis is finished, the pushover curves can be plotted. Pushover curves are plots of the target point displacement versus the base shear in the analyzed direction. The softening of elements which incur in the inelastic range will be reflected on the overall softening of the structure, resulting in a reduced increase of the base shear.

As mentioned before, the main purpose to perform a pushover analysis is because it provides reasonable estimates of location of inelastic behavior. But it is important to recognize that the purpose of pushover analysis is not to predict the actual response of a structure to an earthquake, since it is unlikely that pushover analysis can predict the response (FEMA-451, 2006). Another obstacle mentioned by Lawson et al. (1994), cited by Elnashai (2001), is that it "has no theoretical background and will provide approximate information at best".

Despite the previous mentioned downturns, a pushover analysis was performed in order to identify possible locations of inelastic behavior of the structure during an earthquake. As aforementioned, this type of analysis is mostly used in multistory frame buildings. But in this case, the structure analyzed is a single story highly unsymmetrical structure, in which the lateral loads can not be distributed per story. Therefore, a lateral mass proportional load was applied in both main directions. This is a reasonable approach, since the mass proportional lateral loading represents the inertial forces expected in the building during an earthquake.

7.1 Application to the Safi cathedral

A finite element (FE) analysis of the entire structure was performed. This 3D model is intended for evaluation of the seismic structural safety. Since this 3D model has some border conditions (orthogonal walls, vault) which favors the behavior of the arches, an additional model was made. This corresponds to a plane-stress 2D model of the section of the main arch. This allows comparing the results obtained through the SLOTA whith those of a FE analysis.

1   In a first stage FE phase analyses of the several structural construction steps which the structure will

2   undergo during the restoration project was executed. Starting from the previous mentioned results, a

3   pushover analysis of the entire structure in its final stage was performed

4   Since no mechanical laboratory tests of samples of the old masonry or flat jack tests were carried out,

5   the values chosen for the different parameters of the old masonry correspond to values found in

6   literature. These values have been determined experimentally or have been used in FE models of case

7   studies by various authors. Table 2 shows a summary of the range of mechanical characteristics of

8   different types of stone masonry (but mainly sandstone rubble masonry) which have been determined

9   in-situ or in laboratory conditions. The mechanical characteristics which have been summarized are

10   the Young's modulus (E), the shear modulus (G), the compression strength (f_c), the tensile strength (f_t),

11   the shear strength (τ_u), the Poisson's ratio (ν) and the ultimate tensile strain (ε_u). The mass densities (ρ)

12   of stone masonry have fluctuated in the literature between 1.8 and 2.4 ton/m^3.

13   Based on the previous considerations, values deemed adequate for this case were chosen. The last

14   column of Table 2 shows the values of the mechanical properties chosen to model the masonry. A

15   smear crack model approach was used, due to its computational convenience and its resemblance to

16   the real material. The model was based on a total strain crack model with an ultimate strain based

17   linear softening function in tension. An ideal behavior after reaching the ultimate compressive strength

18   was chosen for the compressive behavior. No lateral confinement behavior and no lateral cracking

19   reduction behavior were used. Additionally, a constant shear retention factor of 0.5 was used. The

20   mass density corresponds to 2.2 ton/m^3.

21   **7.2   The 3D model**

22   Due to the complex nature of the structure and the intervention which it will undergo, the FE model

23   that was created is complex as well. The software used corresponds to DIANA 9.4. The structure was

24   represented through approximately 5200 elements; their types range from linear beams, to triangular

25   shells, to solid cube and wedge elements. The geometry of the cathedral was slightly simplified,

26   though the geometry of the vault is pretty accurate. What makes the modeling of this structure even

more complex is the interaction of elements of different materials, since the original part can be considered as old masonry, while the new gable is of modern reinforced masonry, the walls of the nave and the buttress of reinforced concrete, the truss elements of steel and the roof beams of timber. Although modern materials have higher strength compared with ancient masonry, these materials should also be modeled with non-linear properties in these kind of analysis. All materials present stiffness degradation with increasing loads. For this reason, perfectly elastic materials at the boundaries of old masonry can significantly alter the stress distribution and behavior of masonry. Therefore, the material properties used for the reinforced concrete, steel and timber elements were the ones found in literature for the design of modern constructions. All new materials, except the steel elements, were modeled with ideal behavior after reaching the ultimate tensile and compression strength. A Von Mises material model was used for the steel elements. Additionally, the rebar option of DIANA was used to reinforce the concrete columns.

The results of the pushover analysis are shown in Figure 12 and Figure 13. In this figures the zones with the highest tensile strains also correspond to the zones in which cracking might appear. The figures have been calibrated in such a way that the higher strain levels correspond to a cracking of around 2 mm width or higher. The crack width was determined through integration of the tensile strain levels with respect of a straight line through cracked elements. The target points used are marked with a black dot.

The pushover curve of the analysis in both directions is shown in Figure 14.a. This graph helps us understand the demand the structure can stand, but fails in providing a quantity which indicates in a more illustrative way how the demand relates to the total strength of a structure under a seismic event. If the base shear is divided by the total weight of the structure, a quotient of the lateral mass proportional load is obtained, i.e. the seismic coefficient. This value is equivalent to the fraction of acceleration that is being applied laterally to the structure. This term is often used in literature and is most times displayed as fractions of gravity (g). Figure 14.b shows the pushover curves in terms of seismic coefficient.

1   As it can be seen in Figure 14, the structure stays in the linear range until around 0.28 g in direction -

2   X. This means that the structure would potentially not get damaged during an earthquake with PGA

3   under 0.28 g. The softening of the structure, and therefore potential (partial) collapse, reaches above

4   0.40 g for all directions. The structure can therefore be considered as very robust.

5   It is important to point out that unsymmetrical structures have most likely a direction of action of the

6   loads in which their demand capacity is lower than the other directions. In this study the -X direction

7   turned out to be the weakest. In case retrofitting would be necessary, it would be advisable that the

8   elements which are weaker in this direction, namely the external wall, should be strengthened in order

9   to give them enough resistance to reach the demand capacity that is being predicted for the other three

10   directions, which is over 0.35. But which mechanism will be triggered first also depends on the

11   directionality of the seismic action.

12   If an intervention is necessary depends on the expected demand. Taking into account the arguments

13   exposed before and that the Morocco Seismic Code assumes a PGA of 0.16 g for Safi, a safety factor

14   can be calculated by dividing the lowest PGA in which the structure stays elastic, 0.28 g, by the

15   expected demand for this structure, 0.16 g. This division leads to a safety factor of 1.75. Therefore, no

16   intervention would be necessary, not even for the -X direction.

17   **7.3   The 2D model of the arches**

18   In order to compare the results of a FE model with those of the SLOTA, a plane-stress model of the

19   arch section was made. The deformed shape of the main arch and its tensile strains in the last step of

20   the pushover analysis is shown in Figure 15. As it can be observed in this figure when compared to the

21   results already shown in Figure 11, is that the position of the maximum strains in the arch and the

22   bottom of the supports match approximately the position opposite of the hinges determined in the

23   SLOTA. Therefore, it can be concluded that both methods predict similar collapse mechanisms.

24   The pushover curves of the 2D model are shown and compared to those of the 3D model in Figure 16.

25   As it can be observed in Figure 16.a, the pushover curves between the 2D and the 3D model can not be

26   compared, since the total mass (i.e. the base shear) varies between them. The comparison can only be

made once the base shear is normalized with the total weight of each model, see Figure 16.b. In this case the elastic limit of the pushover curves varies between 0.28 and 0.48 g. In the +X direction the curve of the 2D model resulted lower than the one of the 3D model, because it does not have the support of the orthogonal walls and in this direction the buttress does not give support, since the masonry can crack. On the other hand, in the -X direction the curve of the 2D model is higher than the one of the 3D model. This is due to the support of the buttress in this direction and because in the 3D model, members like the external wall have lesser strength.

In Table 3 the maximum seismic coefficient of the seismic line of thrust analysis are compared to the maximum values obtained in the elastic range of the 2D and 3D pushover analysis. As it can be observed, the values of the SLOTA are more conservative than the ones obtained through the 2D and 3D FE model. On the other hand, the 3D FE model gives more conservatice results than the 2D FE analysis. This is expected, since the 2D model can not capture the weaknesses in the out-of-plane direction.

8. CONCLUSIONS

The Safi Cathedral is an important heritage building and an exceptional witness of the manueline period in midst of the medina of Safi, Morocco. The restoration project foreseen for this monument will introduce modifications to the structure in order to transform it into a museum space. The restoration project will respect the original parts of the structure. This paper dealt with the safety of the cathedral after the restoration project, taking into account the seismic hazard of its region

For this purpose, the modified classical line of thrust method proposed for seismic regions, i.e. SLOTA, was used to asses the safety of arches. This method applies lateral loading on the structure by rotating the lines of action of each element. The method was applied to the section of the arch of the main altar of the cathedral, determining the maximum seismic coefficient.

1   Additionally, a phased 3D pushover FE analysis was done, for which the pushover curves in four

2   directions were determined. This analysis leads to the conclusion that the structure can stand higher

3   lateral loads than the ones expected for this site.

4   The SLOTA resulted easy to implement and is a valuable tool to asses arched structures in a fast and

5   conservative way. On the other hand, the 2D FE analysis is very time consuming, and has the

6   inconvenience that nonlinear material properties have to be defined. This is not always easy, even if

7   experimental or laboratory data is available.

8   Both analyses indicate that the structure is most vulnerable to movements in the +X direction. The

9   SLOTA is more conservative because it did not take into account the upper part of the arch as a

10   structural member, while the 2D FE analysis did. The fact that the line of thrust analysis can account

11   for nonlinear behavior of the material plays also a role. It is difficult to state which one of the

12   approaches is more realistic, since it is not possible to determine if the upper part of the arch acts as a

13   load or as part of the structure. In any case, considering it as a load is on the safe side. To make a real

14   comparison between these two methods, the upper part of the arch could be considered in the SLOTA

15   or the 2D FE model should include interface properties between the elements of the arch and the upper

16   parts of the arch or the structural parts over the arch could be modeled as loads.

17

1

1

REFERENCES

Benouar, D., Molas, G., Yamazaki, F. 1996. Earthquake hazard mapping in the Maghreb countries: Algeria, Morocco, Tunisia. *Earthquake Engineering and Structural Dynamics*, 25, 1151-1164.

Binda, L., Modena, C. 1998. Examples of intervention in ancient constructions. *Structural Analysis of Historical Constructions - Possibilities of numerical and experimental techniques II*, CIMNE, pp 259-286, Barcelona.

Block, P., Ciblac, T., Ochsendorf, J. A. 2006a. Real-time limit analysis of vaulted masonry buildings. *Computers and Structures*, Vol. 84, pp.1841-1852.

Block, P., DeJong, M., Ochsendorf, J. 2006b. As Hangs the Flexible Line: Equilibrium of Masonry Arches. *The Nexus Network Journal*, Vol. 8, No 2, pp 13-24.

Campos, J. 2007. *Impérios, Patrimónios e Identidades*. In Libris, Portugal.

Chiostrini, S., Galano, L., Vignoli, A. 2000. On the determination of strength of ancient masonry walls via experimental tests. *12th World conference on Earthquake Engineering*, Auckland.

Elnashai, A.S. 2001. Advanced inelastic static (pushover) analysis for earthquake applications. *Structural Engineering and Mechanics*, Vol. 12, No. 1, 51-69.

FEMA-356, American Society of Civil Engineers. 2000. Prestandard and Commentary for the Seismic Rehabilitation of Buildings, Federal Emergency Management Agency, Washington, DC.

FEMA-451, NEHRP. 2006. *Recommended Provisions: Design Examples*.

http://www.wbdg.org/ccb/FEMA/fema451.pdf

Henriques at al. 2005. Testing and modeling of multiple-leaf masonry walls under shear and compression. *Structural Analysis of Historical Constructions*, Taylor and Francis Group, London, 2005.

Heyman, J. 1966. The stone skeleton. *International Journal of Solids and Structures*, Vol. 2, 249-279.

Heyman, J. 1995. *The Stone Skeleton: Structural engineering of masonry architecture*. Cambridge: Cambridge University Press.

Heyman, J. 1998. *Structural Analysis - A Historical Approach*. Cambridge University Press.

Huerta, S. 2008. The analysis of masonry architecture: a historical approach. *Architectural Science Review*, Vol 51, 4, pp 297-328.

Kalkan, E., Kunnath, S.K. 2004. Method of modal combinations for pushover analysis of buildings. *13th World Conference on Earthquake Engineering*, August 1-6 of 2004, Paper No. 2713, Vancouver.

Kurrer, K.E. 2008. *The history of the theory of structures: from arch analysis to computational mechanics*. Ernst & Sohn, p.223, Berlin.

Lawson, R.S, Vance. V., Krawinkler, H. 1994. Nonlinear static pushover analysis. Why, when and how? *Proc. of 5th US Nat. Conf. on Earthq. Eng.*, Chicago. 1, 283-292.

Lopez, M. 2004. *A review of existing pushover methods for 2-D reinforced concrete buildings.* A Individual Study Submitted in Partial Fulfillment of the Requirements for the PhD Degree in Earthquake Engineering, European school of advanced studies in reduction of seismic risk.

Lutman, M. 2010. Seismic Resistance Assessment of Heritage Masonry Buildings in Ljubljana. *International Journal of Architectural Heritage*, Vol. 4, Iss. 3, pp 198-221.

Miranda Pires, H. 2009. *Levantamento tridimensional do edifício da Antiga Catedral Portuguesa Safi - Marrocos* (in Portuguese), Portugal.

Oikonomopoulou, A., Ciblac, T., Guéna, F. 2009. Modelling Tools for the Mechanical Behaviour of Historic Masonry Structures. *Proceedings of the Third International Congress on Construction History*, Cottbus, May 2009.

OPCM 3274. 2003. *Norme tecniche per il progetto, la valutazione e l'adeguamento sismico degli edifici* (in Italian, Technical Norms for design, evaluation and seismic rehabilitation of buildings). Ordinanza del Presidente del Consiglio dei Ministri n. 3274 del 20 marzo 2003 e successive modificazioni e integrazioni.

Rao, K., Venkatarama, B., Jagadish, K. Strength characteristics of masonry. 1997. *Materials and Structures*, Vol. 30, pp 233-237.

Ramos, L. 2009. *Relatório da Inspecção Estrutural à Antiga Sé Catedral Portuguesa de Safi – Marrocos* (in Portuguese). Department of Civil Engineering, University of Minho.

Ramos, L.R., Campos, J., Ramos, A., and Marques, F., Sturm, T., Lourenço, P.B.. 2010. Safeguarding of the Portuguese heritage: the case study of Safi Cathedral, Morocco. *Heritage 2010 - Heritage and Sustainable Development Conference,* June 22-26, 1395-1404, Évora, Portugal.

RPS2000 Report, Royaume du Maroc. 2001. *Reglement de Construction Parasismique* (in French). Ministère de l'Aménagement du Territoire, de l'Urbanisme, de l'Habitat et de l'Environnement, Secrétariat d'État à l'Habitat, Rabat.

Sorour, M.M. et al. 2009. Evaluation of Young's Modulus for stone masonry walls under compression. *11th Canadian Masonry Symposium*, pp 121-130, Toronto.

Sturm, T. 2010. *Safety Analysis of the Old Portuguese Cathedral of Safi*. Master Thesis of the Advanced Masters in Structural Analysis of Monuments and Historic Constructions (SAHC), ERASMUS MUNDUS Programme, Universidade do Minho, Portugal.

Sturm, T. 2011. *SLOTA V1.0 - Software manual*. Unpublished, Guimarães, Portugal.

Tomaževič, M. 2010. Heritage masonry buildings and reduction of seismic risk: the case of Slovenia. *Materials, Technologies and Practice in Historic Heritage Structures*, Springer Science+Business Media, pp 327-350.

USGS. 2011. Available at http://earthquake.usgs.gov/earthquakes/world/africa/gshap.php (25/05/2011)

Vintizileu et al. 2006. Mechanical properties of three-leaf stone masonry. *Proceedings of the 5th International conference on Structural Analysis of Historical Constructions - Possibilities of numerical and experimental techniques*, Vol. 2, pp 784-790, New Delhi.

1

2   List of Figures

3

4   Figure 1. Location of the Safi Cathedral in the Medina (Ramos et al., 2010).

5   Figure 2. The cathedral: (a) Plan of street level of the existing structures; (b) possible former outline of

6   the original Cathedral; (c) cross sections of the main altar and the lateral chapel; and (d) plan of the

7   Funchal Cathedral.

8   Figure 3. Main Altar: (a) elevation of main altar in south-west direction; (b) elevation of main altar in

9   north-east direction; (c) inner view of main altar in south-west direction (former hammam); and (d)

10   detail of encounter of pointed arch, diagonal rib and partition wall of south west elevation.

11   Figure 4. General aspects: (a) alley and exterior wall of the Cathedral; (b) north-east façade of the

12   main altar; (c) entrance to the cathedral, through the lateral chapel; and (d) view of the lateral chapel in
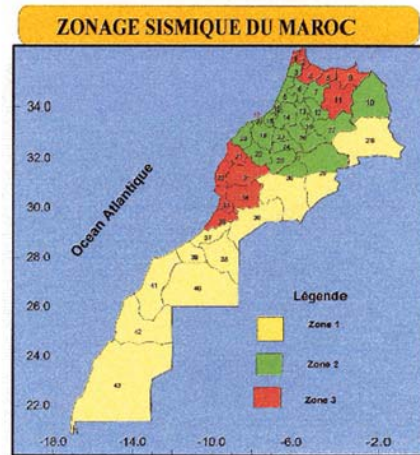
13   direction of the naves.

14   Figure 5. Seimicicy of Morocco: (a) interaction between the African plate and the other plates; and (b)

15   seismic map of Marroco: Zone 1 (Amax/g = 0.01); Zone 2 (Amax/g = 0.08); and Zone 3 (Amax/g =

16   0.16) (RPS2000, 2001).

17   Figure 6. Geographical distribition of seismicity of the Maghreb region during the twentieth centyry,

18   including foreshoocks and aftershocks. (adapted from Benour et al., 1996)

19   Figure 7. Main chapel vault: (a) general view with deflected zone (red); (b) detail of earlier metallic

20   strengthening works, (c) extrados of the vault with vegetation that induces cracks in the cover

21   material; and (d) damage map.

22   Figure 8. Sonic test of the wall: (a) common values for sonic velocities; (b) location of measurement

23   grid; and (c) sonic velocity map.

1   Figure 9. Constructions steps: (a) actual condition; (b) removal of orthogonal wall, construction of the

2   buttress, lateral naves and gable; (c) removal of infill and wall section; and (d) placement of trusses,

3   beams and roof covers.

4   Figure 10. SLOTA: (a) an arch an arch leaning by an angle of α (Block et al., 2006b); and (b) the

5   lines of action of an arch are rotated by an angle of α .

6   Figure 11. Line of thrust of the main arch section: (a) static, without buttress; (b) static, with buttress;

7   (c) seismic in +X direction, $\lambda = 0.175$; and (d) seismic in -X direction, $\lambda = 0.275$.

8   Figure 12. Pushover results; deformed shape and tensile strain (contour levels): (a) direction +X; and

9   (b) direction -X.

10   Figure 13. Pushover results; deformed shape and tensile strain (contour levels): (a) direction +Z; and

11   (b) direction -Z.

12   Figure 14. Pushover curves: (a) base shear; and (b) seismic coefficients.

13   Figure 15. Tensile strains in the section of main arch: (a) pushover in +X direction; and (b) pushover

14   in -X direction.

15   Figure 16. Pushover curves: (a) base shear; and (b) seismic coefficients.

16

1

2 **List of Tables**

3

4 Table 1. Reduction factors of seismic actions (OPCM 3274, 2003).

5 Table 2. Mechanical characteristics of stone masonry determined by various authors.

6 Table 3. Comparison between the seismic coefficients of the SLOTA and the 2D and 3D pushover

7 analysis.

8

9

Figure 1. Location of the Safi Cathedral in the Medina (Ramos et al., 2010).

1

(a)

(b)

(c)

(d)
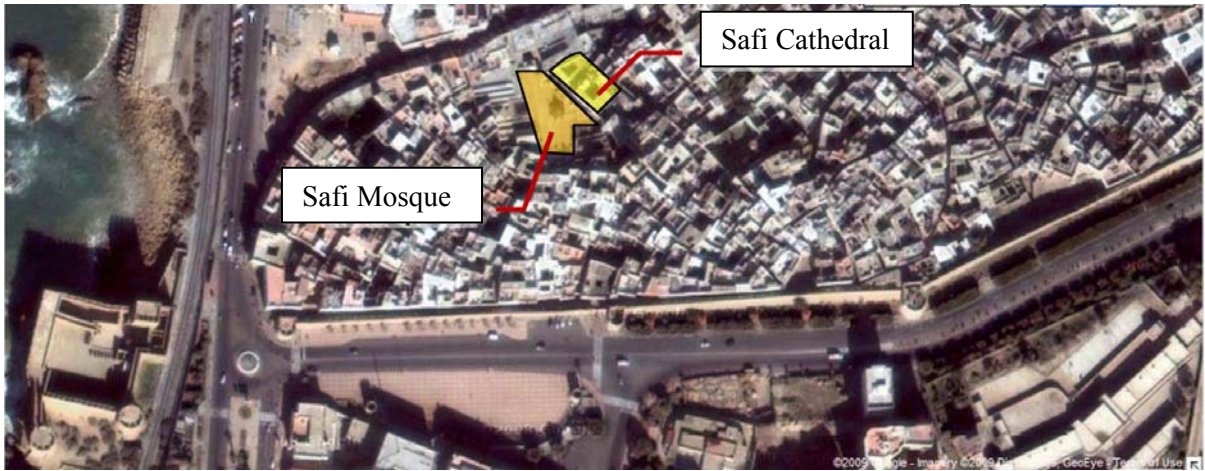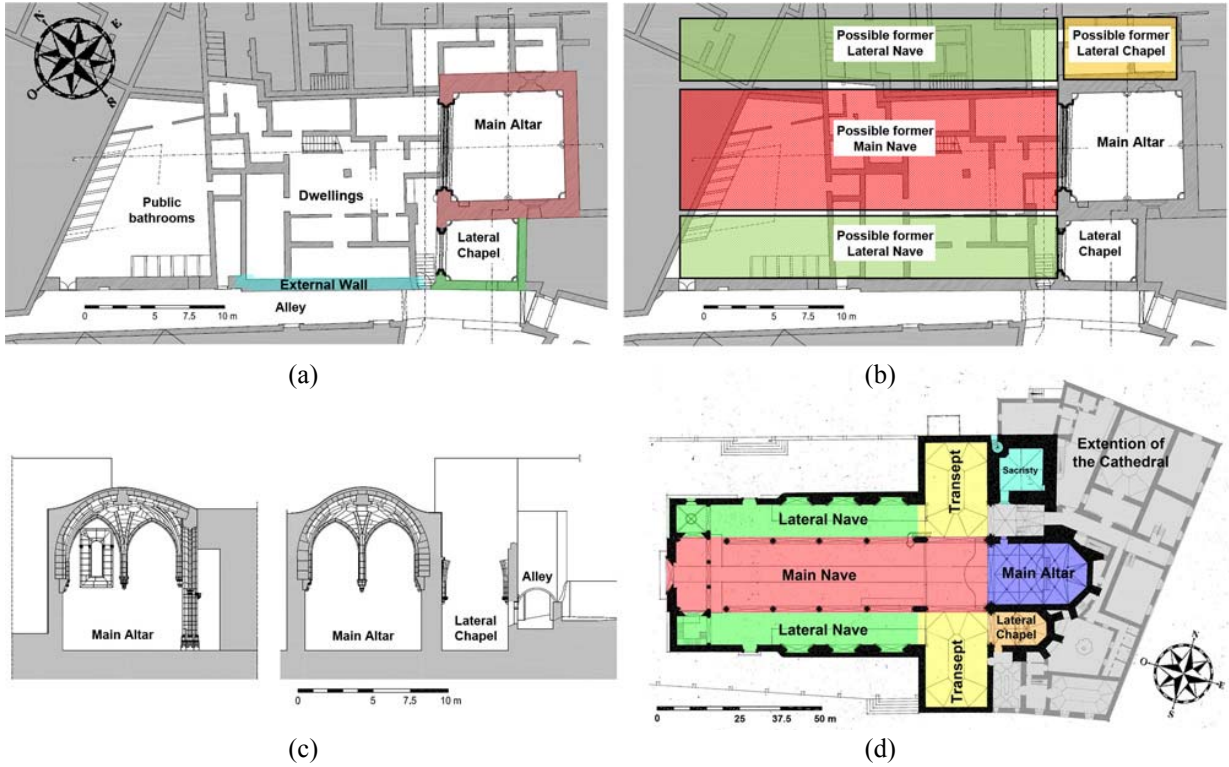
2
3 Figure 2. The cathedral: (a) Plan of street level of the existing structures; (b) possible former outline of the
4 original Cathedral; (c) cross sections of the main altar and the lateral chapel; and (d) plan of the Funchal
5 Cathedral.
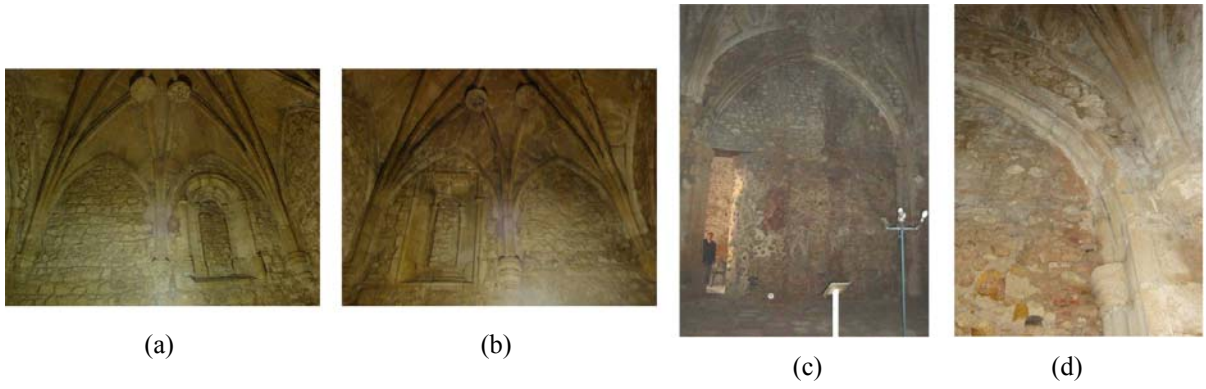
6

1

(a)   (b)   (c)   (d)

2
3   Figure 3. Main Altar: (a) elevation of main altar in south-west direction; (b) elevation of main altar in north-east
4   direction; (c) inner view of main altar in south-west direction (former hammam); and (d) detail of encounter of
5   pointed arch, diagonal rib and partition wall of south west elevation.

6

1
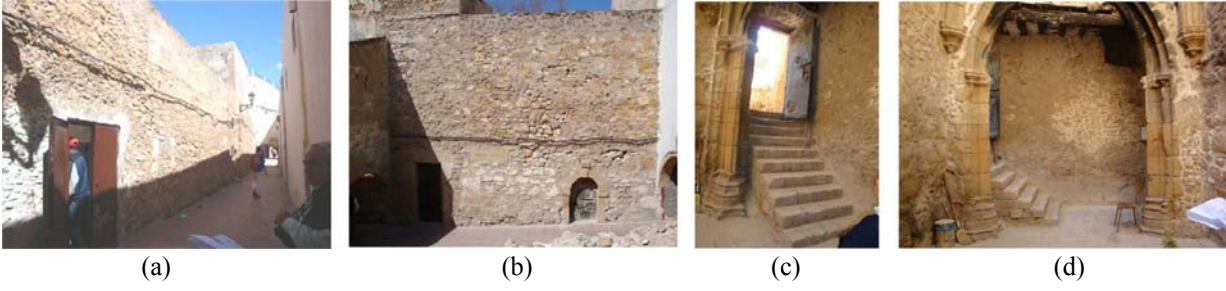
(a)   (b)   (c)   (d)

2
3 Figure 4. General aspects: (a) alley and exterior wall of the Cathedral; (b) north-east façade of the main altar;
4 (c) entrance to the cathedral, through the lateral chapel; and (d) view of the lateral chapel in direction of the
5 naves.
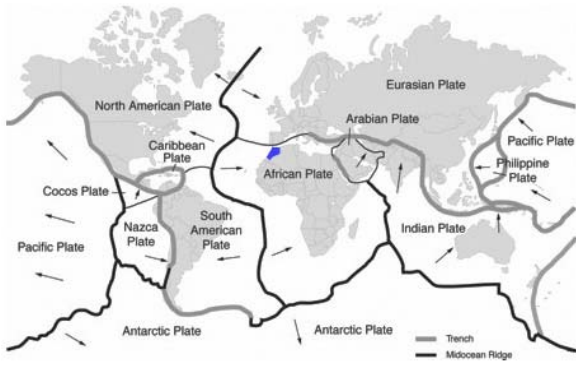
6

1

(a)   (b)

Figure 5. Seimicicy of Morocco: (a) interaction between the African plate and the other plates; and (b) seismic map of Marroco: Zone 1 (Amax/g = 0.01); Zone 2 (Amax/g = 0.08); and Zone 3 (Amax/g = 0.16) (RPS2000, 2001).
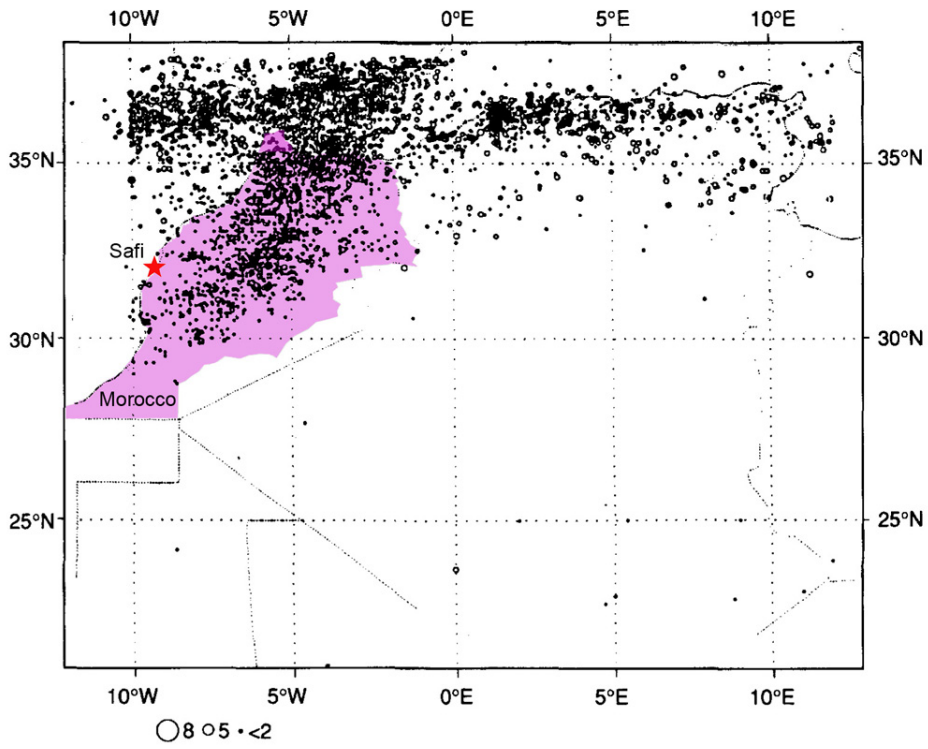
1

2

3

Figure 6. Geographical distribition of seismicity of the Maghreb region during the twentieth centyry, including foreshoocks and aftershocks. (adapted from Benour et al., 1996)

6

1

(a)

(b)

(c)

(d)
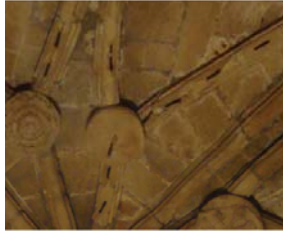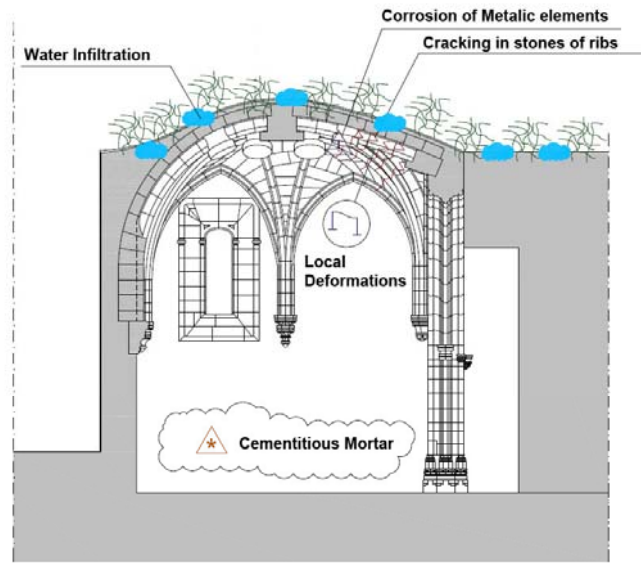
Anomalies:

Water Infiltration / Condensation

Cracks in structural elements

Cracks in structural elements and growth of vegetation

Excessive deformations / Settlement of supports

Deterioration of materials / Corrosion

Other anomalies

2
3 Figure 7. Main chapel vault: (a) general view with deflected zone (red); (b) detail of earlier metallic
4 strengthening works, (c) extrados of the vault with vegetation that induces cracks in the cover material; and (d)
5 damage map.

6

1

Type of material	Sonic velocity [km/s]
Steel	5.8
New masonry	1.0 - 3.0
Old masonry	0.4 - 2.5
Concrete	4.2 - 5.2
Timber	3.5 - 6.0
Stone	2.0 - 5.0
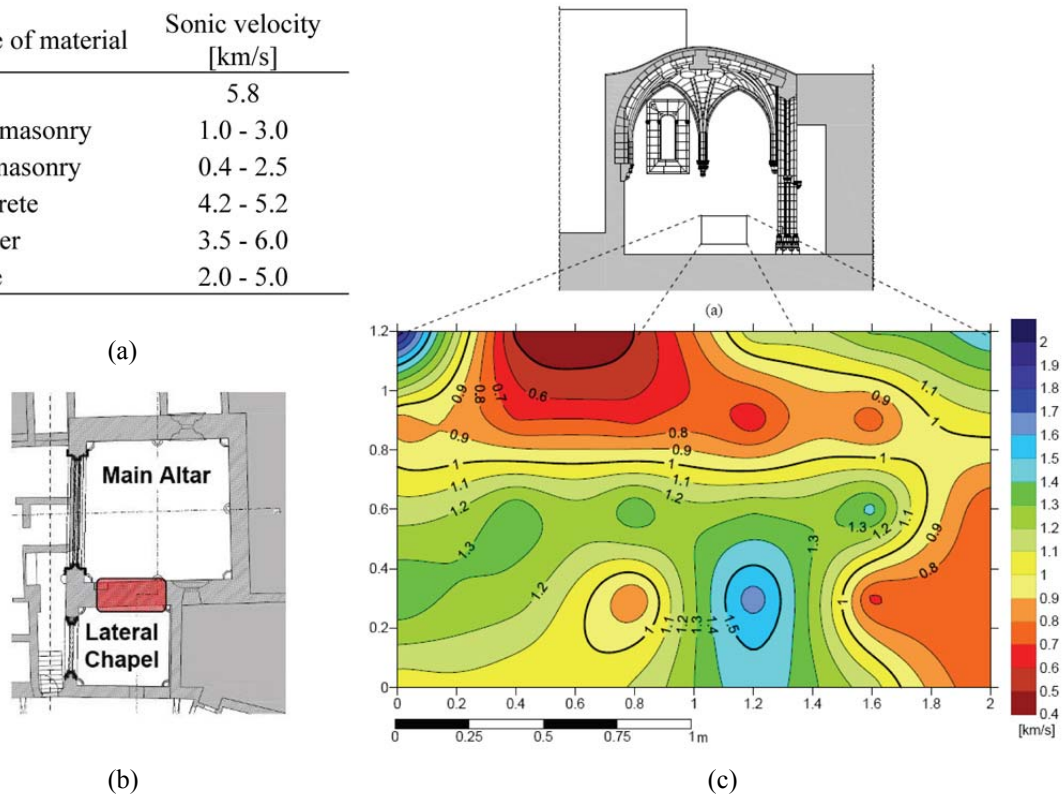
(a)

(b)   (c)

2
3   Figure 8. Sonic test of the wall: (a) common values for sonic velocities; (b) location of measurement grid; and
4   (c) sonic velocity map.
5
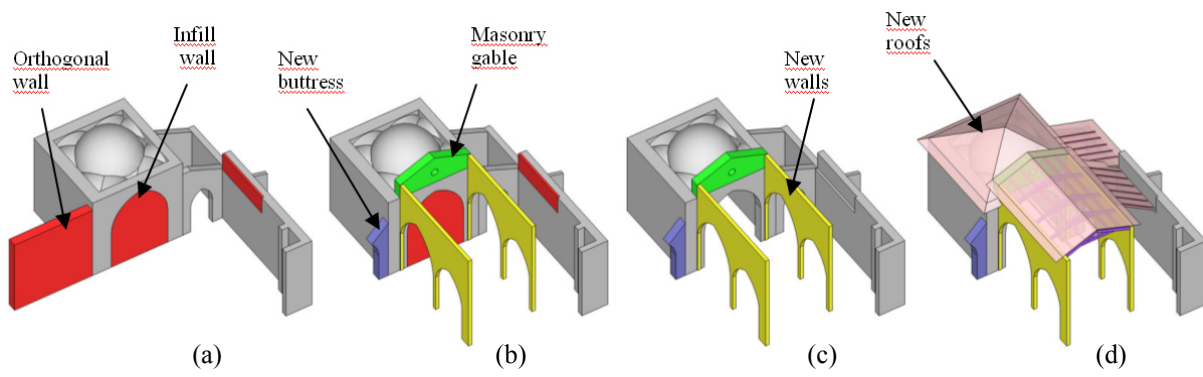
Figure 9. Constructions steps: (a) actual condition; (b) removal of orthogonal wall, construction of the buttress, lateral naves and gable; (c) removal of infill and wall section; and (d) placement of trusses, beams and roof covers.

1

(a)   (b)
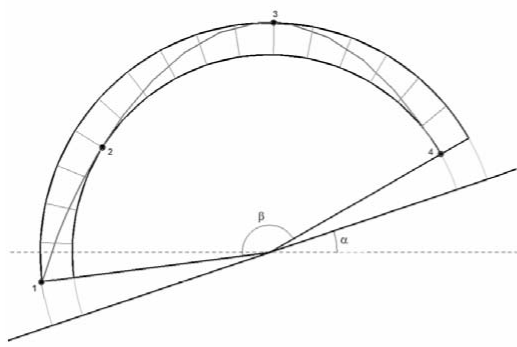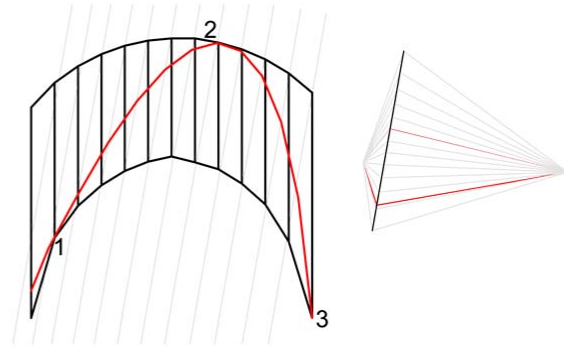
2 Figure 10. SLOTA: (a) an arch an arch leaning by an angle of α (Block et al., 2006b); and (b) the lines of
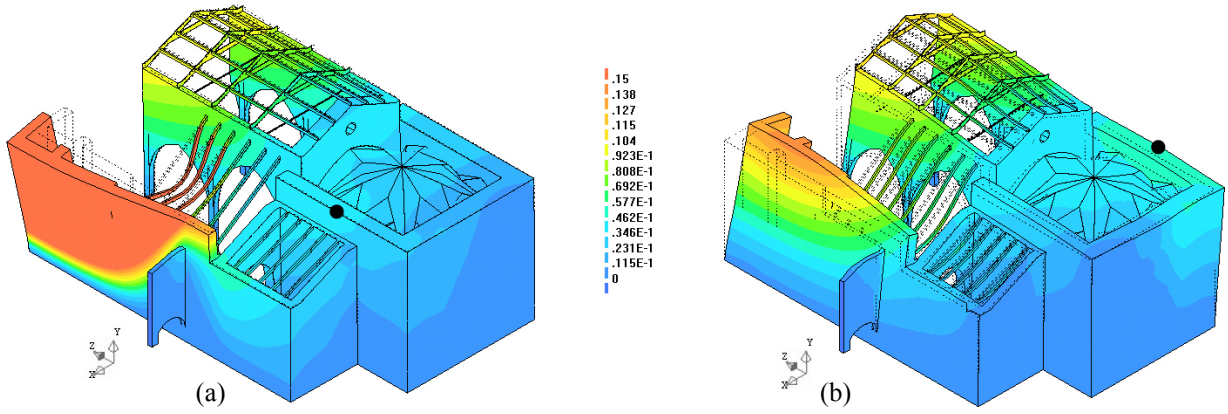3 action of an arch are rotated by an angle of α.
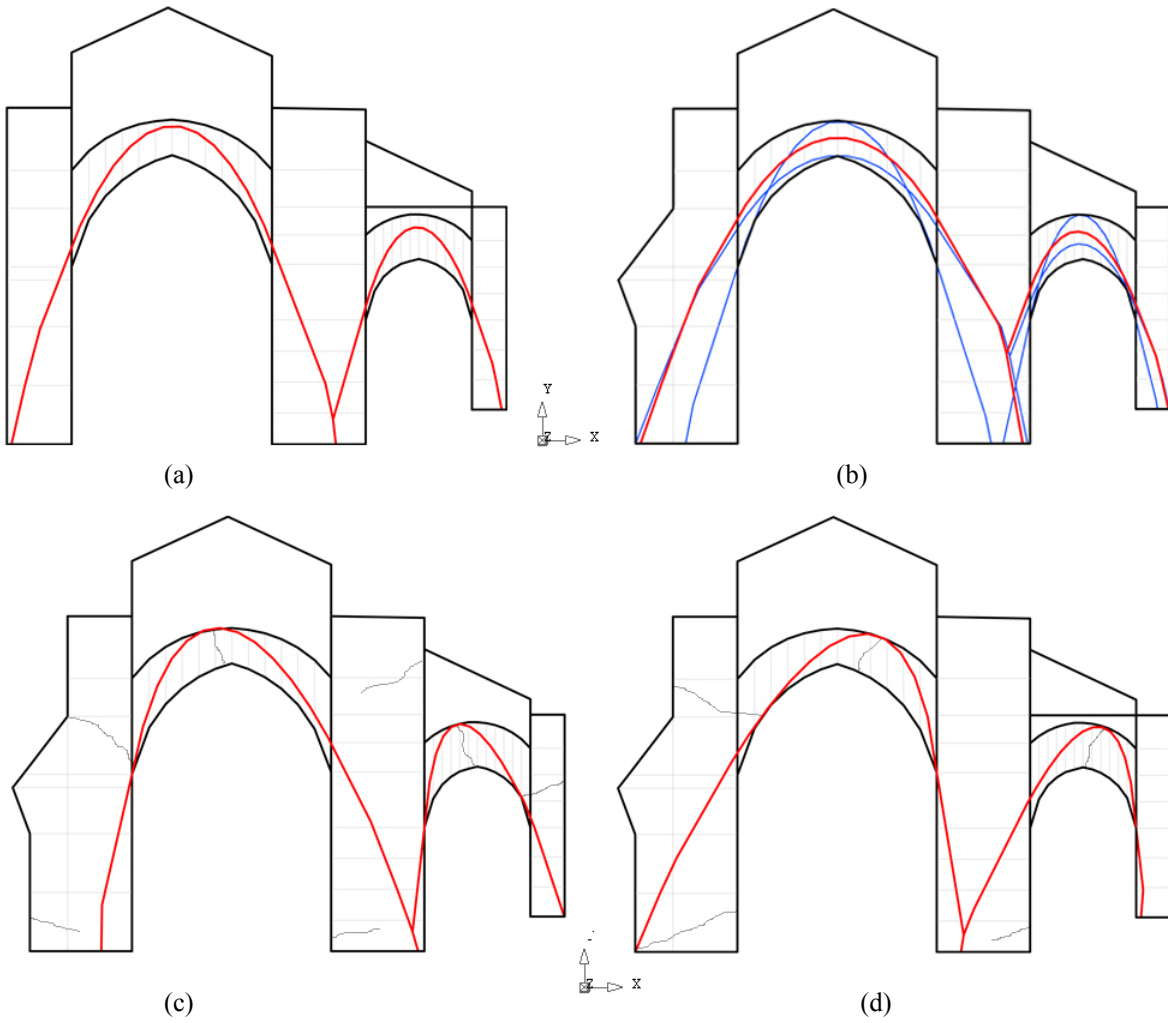
4

Figure 11. Line of thrust of the main arch section: (a) static, without buttress; (b) static, with buttress; (c) seismic in +X direction, λ = 0.175; and (d) seismic in -X direction, λ = 0.275.
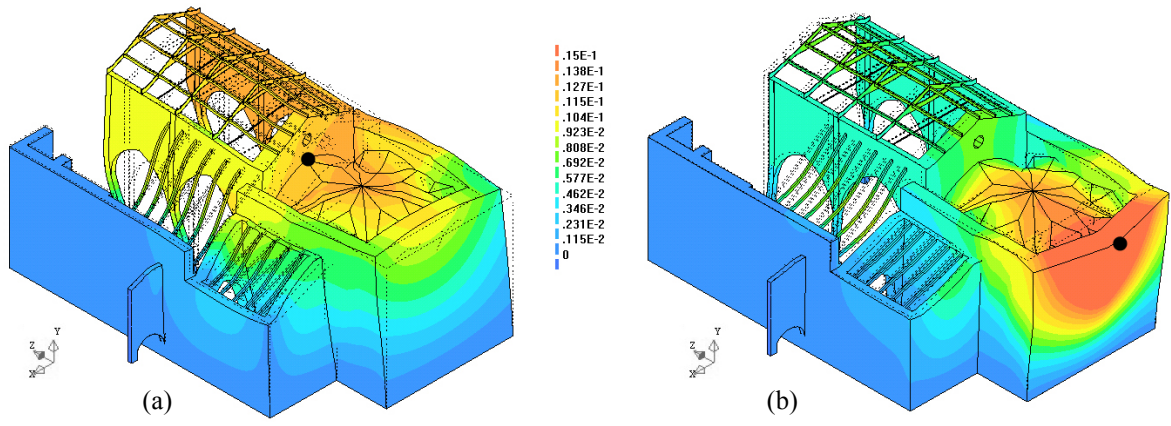
1

(a)	(b)

2
3 Figure 12. Pushover results; deformed shape and tensile strain (contour levels): (a) direction +X; and (b)
4 direction -X.
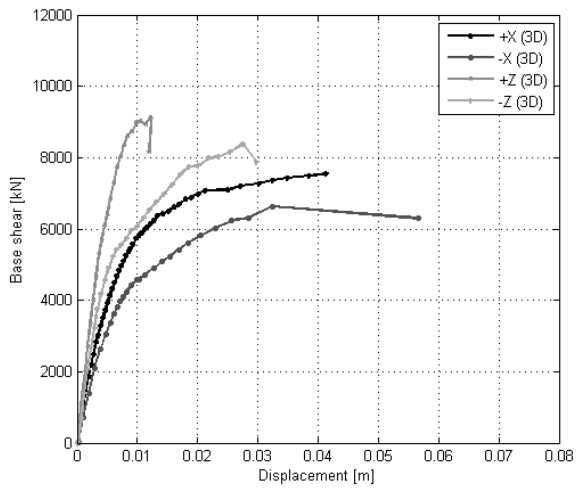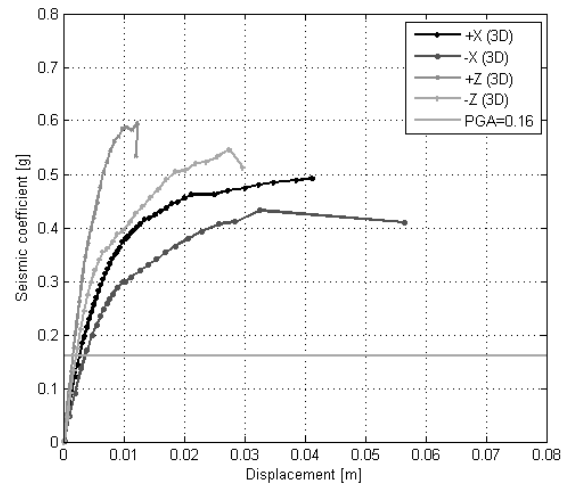
5

1

2 Figure 13. Pushover results; deformed shape and tensile strain (contour levels): (a) direction +Z; and (b)
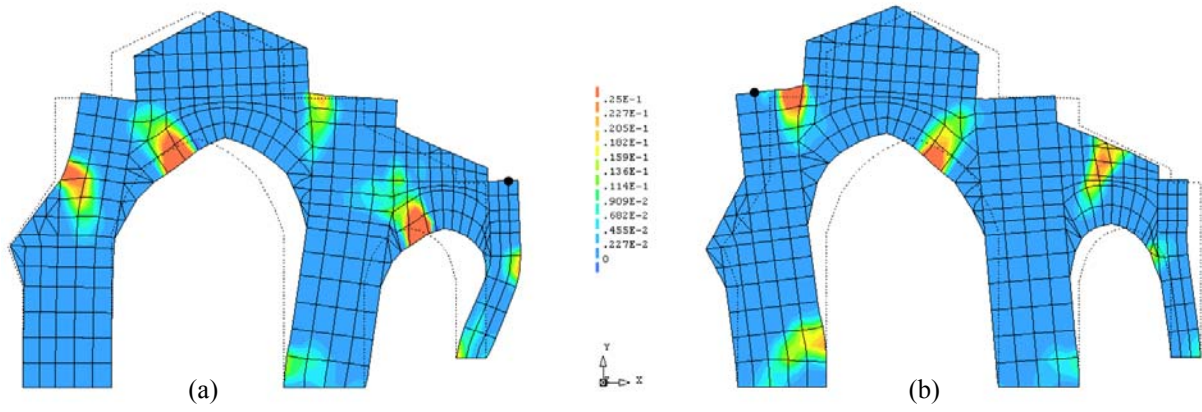3 direction -Z.

4

<div style="text-align:center">(a)   (b)</div>
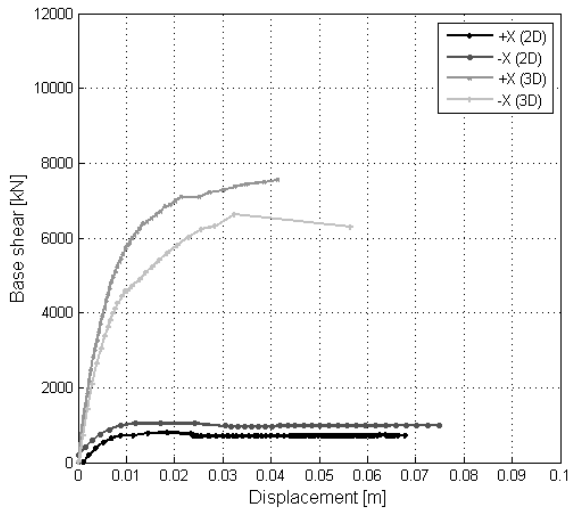
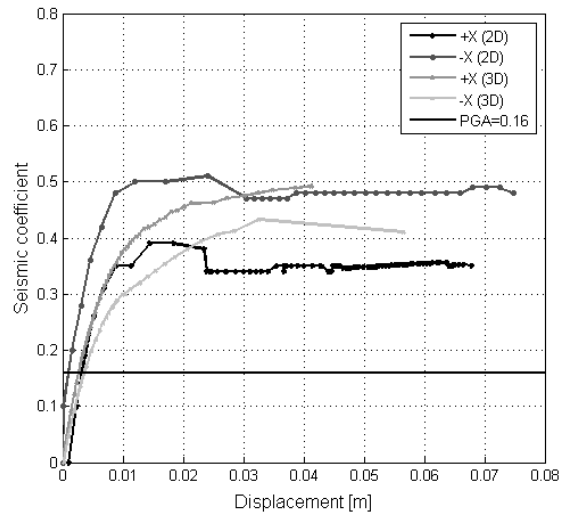Figure 14. Pushover curves: (a) base shear; and (b) seismic coefficients.

Figure 15. Tensile strains in the section of main arch: (a) pushover in +X direction; and (b) pushover in -X direction.

(a)

(b)

Figure 16. Pushover curves: (a) base shear; and (b) seismic coefficients.

1   Table 1. Reduction factors of seismic actions (OPCM 3274, 2003).

Category of use	Relevance Category		
	Limited	Average	High
Irregular or not used	0.50	0.65	0.80
Frequent	0.65	0.80	1.00
Daily	0.80	1.00	1.20

2

3

1   Table 2. Mechanical characteristics of stone masonry determined by various authors.

Material Properties	Chiostrini et a.l (2000)	Rao et al. (1997)	Henriques et al. (2005)	Sorour et al. (2009)	Tomaževič (2010)	Lutman (2010)	Binda & Modena (1998)	Vintzileou et al. (2006)	Adopted values
E [GPa]	–	–	1770 - 2720	1900	321 - 390	–	470 - 1380	1000 - 1500	1000
G [GPa]	140 - 360	–	–	–	65 - 170	–	–	–	–
f_c [MPa]	–	0.71 - 0.98	5.8 > 15.1	1.50	0.33 - 0.98	0.9 - 3.0	1.87-2.26	1.74-2.26	1.00
f_t [MPa]	–	0.6 -1.4	0.09 - 0.14	–	0.02 - 0.32	0.04 - 0.18	–	~0.10	0.10
τ_u [MPa]	0.07 - 0.23	–	0.08-0.09	–	–	–	–	–	–
ν	–	–	0.10 - 0.15	0.25	–	–	0.07 - 0.20	–	0.2
ε_u	–	–	-	<0.003	–	–	–	<0.0016 - 0.0026	0.004
Type of results	In-situ	Lab.	Lab.	Lab.	In-situ	Ref. of Buildings	Double flat-jack	Lab.	Model

2
3

1   Table 3. Comparison between the seismic coefficients of the SLOTA and the 2D and 3D pushover analysis.

Direction	SLOTA	2D model	3D model
+X	0.175	0.31	0.28
-X	0.275	0.48	0.37

2